

Post-Print of: J. Exp. Bot. (2011) 62 (13): 4547-4559.

## **Integrated functions among multiple starch synthases determine both amylopectin chain length and branch linkage location in Arabidopsis leaf starch**

Nicolas Szydlowski 1, Paula Ragel 2, Tracie A. Hennen-Bierwagen 3, Véronique Planchot 4, Alan M. Myers 3, Angel Mérida 2, Christophe d'Hulst 1 and Fabrice Wattebled 1,†

1 Unité de Glycobiologie Structurale et Fonctionnelle, UMR8576 CNRS-Université Lille 1, sciences et technologies, F-59655 Villeneuve d'Ascq, France

2 Instituto de Bioquímica Vegetal y Fotosíntesis, Consejo Superior de Investigaciones Científicas-Universidad de Sevilla, Isla de la Cartuja, E-41092-Seville, Spain

3 Department of Biochemistry, Biophysics, and Molecular Biology, Iowa State University, Ames, Iowa 50011, USA

4 UR1268 Biopolymères, Interactions, Assemblages, INRA France, F-44300 Nantes Cedex 3, France

### **Abstract**

This study assessed the impact on starch metabolism in Arabidopsis leaves of simultaneously eliminating multiple soluble starch synthases (SS) from among SS1, SS2, and SS3. Double mutant *ss1- ss2-* or *ss1- ss3-* lines were generated using confirmed null mutations. These were compared to the wild type, each single mutant, and *ss1- ss2- ss3-* triple mutant lines grown in standardized environments. Double mutant plants developed similarly to the wild type, although they accumulated less leaf starch in both short-day and long-day diurnal cycles. Despite the reduced levels in the double mutants, lines containing only SS2 and SS4, or SS3 and SS4, are able to produce substantial amounts of starch granules. In both double mutants the residual starch was structurally modified including higher ratios of amylose:amylopectin, altered glucan chain length distribution within amylopectin, abnormal granule morphology, and altered placement of  $\alpha(1\rightarrow6)$  branch linkages relative to the reducing end of each linear chain. The data demonstrate that SS activity affects not only chain elongation but also the net result of branch placement accomplished by the balanced activities of starch branching enzymes and starch debranching enzymes. SS3 was shown partially to overlap in function with SS1 for the generation of short glucan chains within amylopectin. Compensatory functions that, in some instances, allow continued residual starch production in the absence of specific SS classes were identified, probably accomplished by the granule bound starch synthase GBSS1.

### **Key words**

Amylopectin, amylose, branching, chain-length-distribution, glucans, SS1, SS2, SS3, starch, starch synthases

## Introduction

Semi-crystalline starch granules are a hallmark of plant metabolism, allowing long-term storage of photosynthate in both leaves and seeds. Starch granules are composed of two types of structurally distinct  $\alpha$ -glucan polymer, amylose and amylopectin, in which linear chains of  $\alpha(1\rightarrow4)$ -linked glucose units are branched through  $\alpha(1\rightarrow6)$  bonds (Buleon et al., 1998). Amylose has an amorphous structure, is branched at a very low frequency, and not mandatory for granule formation. Amylopectin differs from amylose in that it is semi-crystalline, moderately branched with 5-6%  $\alpha(1\rightarrow6)$  linkages (Buleon et al., 1998), and provides the essential structure of the starch granule. The architectural arrangement of glucose units within amylopectin differs from that of soluble glucan storage polymers, i.e. glycogen, particularly regarding linear chain length distribution and branch linkage location. How such architectural specificity is attained enzymatically is not well understood.

Although some specific features differentiate transitory (in source organs such as leaves) and storage (in sink organs such as tubers and seeds) starch metabolisms, the model land plant *Arabidopsis* is essentially typical of all Chloroplastida with regard to its complement of starch biosynthetic enzymes (Zeeman et al., 2002). Starch is synthesized by the concerted activities of three different enzymes, specifically (i) starch synthase (SS), elongating enzymes that transfer glucose moieties from ADP-glucose to growing  $\alpha$ -glucans by the formation of a new  $\alpha(1\rightarrow4)$  glycoside bond; (ii) starch branching enzymes (BE) that introduce  $\alpha(1\rightarrow6)$  bonds by inter- or intra-molecular rearrangement of pre-existing linear chains; and (iii) starch debranching enzymes (DBE) that hydrolyse some of the branches previously introduced in the structure by BE, presumably allowing crystallization and further growth of the molecules (Ball et al., 1998; Myers et al., 2000; Deschamps et al., 2008). The interactions of SS, BE, and DBE that establish amylopectin structure are inherently complex owing to cyclic substrate-product relationships. For example, linear chains produced by SS are substrates of BE, and short chains with 6–7 glucose units generated during branch formation are, in turn, substrates of SS (Zeeman et al., 2007; Liu et al., 2009, and references therein). The products of BE are also substrates of DBE. In addition, SS activity also may influence substrate structure for DBE, because some members of this enzyme class hydrolyse specific branch lengths (Dauvillee et al., 2005).

Five classes of SS gene were established early in the evolution of chloroplast-containing organisms, including green algae and land plants (Deschamps et al., 2008). Phylogenetic relationships demonstrate that each gene was functionally selected rather than having evolved from relatively recent gene duplications. The specific functions of each SS class in starch biosynthesis, however, remain for the most part unexplained. Granule-bound starch synthase (GBSS) may be a relatively straightforward example, because genetic analyses indicate that amylose synthesis is strictly dependent upon this class and does not specifically require any of the four SSs that occur in the soluble phase. By contrast, at least four SS classes, referred to as SS1 to SS4, are involved in the synthesis of amylopectin. Two phylogenetically distinct classes of BE are for the most part conserved in all Chloroplastida, and in most instances the BEII class is represented by two different enzymes generated by gene duplication. *Arabidopsis* is an exception to this general rule because it lacks any gene coding for BEI. DBEs are encoded by four highly conserved genes present in all Chloroplastida examined to date, including both green algae and land plants. Much remains to be discovered in order to explain the presence

of starch in chloroplast-containing organisms, including the functional interactions between SS, BE, and DBE, and the specific functions of the multiple classes of each enzyme responsible for their extremely broad conservation.

Genetic analyses have been useful in identifying functions of specific SS classes. The structure of amylopectin from mutant *Arabidopsis* lines indicates that SS1 is mainly involved in the synthesis of shorter chains up to about DP 10 (Delvallé et al., 2005), whereas SS2 is necessary to generate chains of up to about DP 20 (Zhang et al., 2008). SS1 and SS2, therefore, together generate chains that, according to the Hizukuri model of amylopectin structure, comprise the crystalline lamellae (see Supplementary Fig. S1 at JXB online) (Hizukuri, 1986). A straightforward relationship can be envisioned in which SS1 generates DP 6–10 glucans and then SS2 elongates those to about DP 12–20. Single mutant data, however, rule out this hypothesis. If SS1 were needed to generate short chains first, then that mutation should essentially prevent amylopectin synthesis. Instead, SS1 mutants have a near-normal starch content in which the chain length distribution is shifted towards longer chains generated by SS2. This indicates a negative influence of SS1 on SS2 activity, potentially by competition for substrate binding, or direct regulatory interactions within protein complexes containing multiple SS classes (Hennen-Bierwagen et al., 2008, 2009; Tetlow et al., 2008; Liu et al., 2009). SS3 appears to be responsible for the synthesis of longer glucans that run between two or more clusters, however, this isoform also provides some functions that overlap with SS2 to generate single-cluster chains (Zhang et al., 2005, 2008). SS4 is not required for normal amylopectin structure but rather appears to be an important factor in granule initiation (Roldán et al., 2007), and SS3 also provides overlapping function in this process (Szydlowski et al., 2009). SS4, however, is able to support synthesis of some level of residual starch granules when it is the only SS present, indicating it can contribute to amylopectin structure in some conditions (Szydlowski et al., 2009).

To define the functions of the conserved SS classes further, this study generated *Arabidopsis* lines lacking both SS1 and SS2, or SS1 and SS3. In the first instance, the remaining classes, SS3 and SS4, can sustain the synthesis of nearly normal levels of starch, suggesting that SS3 provides partially overlapping functions in the generation of clusters. In lines containing only SS2 and SS4 there is a strong reduction in starch content, indicative of an SS3 function in generating the linked clusters necessary for substantial granule growth. The effects of the double mutations on total SS activity in soluble extracts were synergistic, indicating functional interactions between the classes. The placement of branch linkages was substantially different in either double mutant compared with the wild type, which provides a clear indication that the activity of SS influences not only the length of the glucan chains in amylopectin, but also the placement of branch linkages. Thus, co-ordinated actions of Ss with BEs and/or DBEs generate the normal amylopectin structure.

## **Materials and methods**

### **Generation of *Arabidopsis* lines**

All *Arabidopsis* lines used in this study were in the WS genetic background. Plants were grown either in a greenhouse (16/8 h light/dark; with 24 °C during the day, 18 °C at night; 150  $\mu\text{mol photon m}^{-2} \text{s}^{-1}$ ; 60% humidity) or in controlled-environment chambers (12/12 h light/dark;

with 23 °C during the illuminated phase, 19 °C at night; 100  $\mu\text{mol photon m}^{-2} \text{s}^{-1}$ ; 75% humidity). Double heterozygotes were generated by crosses between single mutants containing *ss1-1* (Delvallé et al., 2005) and either *ss2-3* (Zhang et al., 2008) or *ss3-3* (Szydlowski et al., 2009). The latter allele was previously referred to as *ss3-2*, but that designation has been changed to distinguish it from the *ss3-2* mutation previously described in the Columbia genetic background (Zhang et al., 2005). Double heterozygous lines were selected by PCR amplification of the relevant wild-type and mutant alleles from genomic DNA, using specific primers as previously described (Delvallé et al., 2005; Zhang et al., 2008; Szydlowski et al., 2009) (see Supplementary Fig. S2 at JXB online). The selected lines were allowed to self-pollinate. These seeds were then sown and double mutant plants were identified using PCR amplification to determine the genotype. Self-pollination of those plants provided a stock of homozygous double mutant seed used to generate plants for subsequent analyses.

Isolation of genomic DNA from leaf tissue and PCR amplification were performed according to standard procedures described previously by Wattebled et al. (2008). PCR primers used for mutant allele identification hybridize to the T-DNA left border (Tag5, 5'-CTACAAATTGCCTTTTCTTATCGAC), and to genomic sequences of the *SS1* (*ss1rev*, 5'-TACGCCAAAGTCAGCCATTACAA), *SS2* (*ss2rev*, 5'-CGGTCGCCCTGTGCCTAAC) or *SS3* (*ss3rev*, 5'-CTTGAGCTTGTGCCCTTTCTTTAT) genes. PCR primer pairs used for wild-type allele amplification hybridize on both sides of the T-DNA insertion position. *SS1* was amplified using *ss1rev* and *ss1for* (5'-TTTCCGTCGATCGCCAGTCTC), *SS2* was amplified using *ss2rev* and *ss2for* (5'-GGGGACCGGTAGATGATTC), and *SS3* was amplified using *ss3rev* and *ss3for* (5'-GTTCTTTATTTGCTGTCCGTATT).

### **In vitro assays of starch metabolizing enzymes**

Quantitative analysis of  $\alpha$ -amylase, pullulanase,  $\alpha(1\rightarrow4)$  glucanotransferase, and  $\alpha$ -glucosidase activities in total soluble leaf extracts were determined as previously described by Zeeman et al. (1998). ADP-glucose pyrophosphorylase activity was assayed in the degradation direction, in the presence or absence of 3-PGA, according to the method described by Delvallé et al. (2005).

*SS* activity was measured essentially as previously described by Delvallé et al. (2005), with the following details. Leaf extract (125  $\mu\text{g}$  protein) was incubated for 30 min at 30 °C with 1 mM ADP-[U14C]glucose (3.7 GBq mol<sup>-1</sup>) and 1% glycogen (Sigma-Aldrich) in 100 mM tricine, pH 8.0, 25 mM potassium acetate, 5 mM EDTA, 10 mM DTT, 0.05% BSA. Reactions were stopped by boiling for 5 min. Polysaccharides were precipitated in 75% methanol, 1% KCl and then washed three times with the same solution. Pellets were suspended in distilled water and incorporated radioactivity was measured with a scintillation counter.

*BE* activity was determined as described previously by Dumez et al. (2006), as follows. Leaf extract (100  $\mu\text{g}$  protein) was incubated for 30, 45 or 60 min at 30 °C in a final volume of 200  $\mu\text{l}$  of 100 mM sodium citrate buffer, pH 7.0, 1 mM AMP, 50 mM [U14C]-Glc-1-P (50 dpm nmol<sup>-1</sup>) and 3.2 U of phosphorylase a (Sigma-Aldrich). Glycogen was added as a carrier (100  $\mu\text{l}$  of a 1% solution) and reactions were then stopped by boiling for 5 min. Glucans were precipitated and incorporated radioactivity was quantified as for the *SS* assay.

### **Zymogram techniques**

Soluble starch synthases, starch-modifying activities, starch phosphorylases, phosphoglucomutases, and pullulanase zymograms were performed as described by Delvallé et al. (2005). Zymograms to reveal  $\beta$ -limit dextrin-modifying activities were performed using 100  $\mu$ g protein from a leaf crude extract separated by native PAGE (7.5% acrylamide) containing 0.2% maize  $\beta$ -limit dextrin. After migration for 3 h at 4 °C at 15 V cm<sup>-1</sup>, the gel was incubated overnight at room temperature in 100 mM TRIS-HCl, pH 7.0, 1 mM MgCl<sub>2</sub>, 1 mM CaCl<sub>2</sub>, 1 mM DTT, and then stained with iodine.

### **Starch content and structure**

Methods used for the analysis of starch content and structure have been described previously. These include starch granule purification and determination of leaf starch content (Wattebled et al., 2005), solubilization of starch and separation of amylose and amylopectin by size exclusion chromatography on Sepharose CL-2B (Delvallé et al., 2005), debranching of amylopectin with *Pseudomonas* isoamylase and determination of chain length distribution by HPAEC-PAD (Wattebled et al., 2005), conversion of amylopectin to  $\beta$ -limit dextrin (Delvallé et al., 2005), scanning electron microscopy (SEM), and embedding, sectioning, and imaging by transmission electron microscopy (TEM) (Delvallé et al., 2005).

## **Results**

### **Leaf starch content**

The alleles utilized in this study were *ss1-1* (Delvallé et al., 2005), *ss2-3* (Zhang et al., 2008), and *ss3-3* (Szydlowski et al., 2009) (previously designated *ss3-2*), all of which were shown previously to be null mutations. Double mutant lines in the WS genetic background were constructed by standard methods, and the presence of each allele was verified by PCR analysis of genomic DNA (see the Materials and methods). Activities of SS1 and SS3 were visualized by zymogram and the presence or absence of the *ss1*- and/or *ss3*- mutations in each line was confirmed by the appearance or absence of the appropriate activity band (Fig. 1A). Plants were grown either in long-day conditions in the greenhouse (LD; 16/8 h light/dark) or short-day conditions in controlled-environment chambers (SD; 12/12 h light/dark). The double mutant lines were analysed in comparison to wild-type WS and each single mutant for seed germination, plant growth, flowering time and rate, and silique formation. No obvious growth or developmental differences were observed between the wild type, *ss1*-, *ss2*-, *ss3*-, *ss1- ss2*-, and *ss1- ss3*- plants.

Leaf starch content at the end of the light period was compared between the wild type and the double-mutant lines grown under LD or SD conditions (Fig. 2). Such analyses of single mutants were previously published but were repeated in this study to allow direct comparison and to minimize potential environmental effects. Starch content was normal in either *ss1*- or *ss2*- single mutants grown in LD conditions. In SD conditions the *ss1*- mutant had about 70% of the wild-type starch level, and the *ss2*- mutant was more severely affected, accumulating only 40% of the normal amount. The *ss3*- mutant line accumulated 80% of the wild-type starch level at the end of the light period in either LD or SD conditions.

In LD conditions the *ss1- ss2-* double mutant was not significantly decreased in starch content compared with the wild type or either single mutant (Fig. 2). Therefore, SS3 appears to provide sufficient function to produce essentially the same amount of starch found in the wild type, presuming that SS4 is involved exclusively in granule initiation as has been proposed by Roldán et al. (2007). A light phase of at least 16 h is necessary for the generation of normal starch levels using only SS3 and SS4, because the *ss1- ss2-* double mutant is decreased by 30% from the wild-type content in SD conditions. A notable observation is that in SD conditions the starch content of the *ss1- ss2-* double mutant is greater than that of the *ss2-* single mutant. In fact, the double mutation reflected the starch content of the *ss1-* mutation alone and appeared to negate the contribution of the *ss2-* deficiency.

The *ss1- ss3-* double mutant had only 60% of the wild-type starch level in LD conditions. This result may indicate a synergistic relationship between SS1 and SS3, because the *ss1-* line was not decreased in starch content and the *ss3-* single mutant was decreased only by 20%. By contrast, the effects of the *ss1-* and *ss3-* mutations appear to be additive in SD conditions.

### **Starch metabolic enzyme activities**

Zymogram analyses were used to examine comprehensively the effects of the double mutations on enzymes involved in starch metabolism. Based on these qualitative assays, the activities of starch biosynthetic enzymes other than SS were not affected in any single- or double mutant line (Fig. 1). The enzymes thus examined were isoamylase-type DBE (ISA), pullulanase-type DBE (PUL), SBE2, SBE3, phosphoglucomutases, and the  $\beta$ -amylase RAM1 (Laby et al., 2001). Quantitative assays of enzyme activities in total soluble leaf extracts from plants grown in LD conditions and harvested in the middle of the light period were also performed (Table 1). Significant differences from the wild type were not observed in any line for the enzymes ADPGlc pyrophosphorylase, pullulanase, disproportionating enzyme (D-enzyme), maltase, or  $\alpha$ -amylase. Relatively slight increases in total SBE activity in the double mutants were detected, however, this assay is indirect (it is based on the stimulation of phosphorylase 'a' polymerizing activity in the presence of high concentration of Glc-1-P) and the magnitude of the increase is not likely to reflect a considerable change *in vivo*.

The residual level of total soluble SS activity was about 25% of normal in the *ss1- ss2-* double mutant, and about 10% of WT in the *ss1- ss3-* double mutant. Notably, the drop of SS activity in both double mutants does not match the addition of the reduction measured in the corresponding single mutants. For example, *ss1-* single mutants exhibit approximately 50% of the wild-type total soluble SS level and *ss2-* single mutant lines are not affected in this parameter. The double mutant, however, exhibits 75% less total soluble SS activity than the wild type. Similarly, *ss3-* single mutants have less than 10% reduction of SS activity, yet the *ss1-ss3-* line is about 90% reduced. Thus, there appear to be compensating mechanisms or other, as yet uncharacterized, regulatory interactions that occur between soluble SS classes.

### **Starch composition and size distribution of linear glucans in amylopectin**

Amylose (low mass fraction) and amylopectin (high mass fraction) from starch solubilized in 10 mM NaOH were separated by size exclusion chromatography (Fig. 3) using Sepharose® CL-2B matrix. The amylose content was measured both as a percentage of total glucan in the

granules and normalized to fresh leaf weight (Table 2). As reported previously (Zhang et al., 2008), the content of the low mass fraction of starch was significantly elevated in *ss2*- single mutant plants both as a percentage of the total glucan in starch and as a function of fresh leaf weight. This effect was enhanced in the *ss1*- *ss2*- double mutant, even though the *ss1*- mutation by itself has no effect on the amount of this fraction of starch (Table 2). The presence of this low mass fraction in the *ss2*- mutant is strictly under the control of GBSS1 because it is entirely lacking in the *gbss1*- *ss2*- double mutant (see Supplementary Fig. S3 at JXB online). It could therefore be considered as true amylose since the synthesis of this fraction of starch is exclusively under the control of GBSS1 activity. Although it is likely that the same applies for the *ss1*- *ss2*- mutant, it cannot definitely be concluded that the low mass fraction is strictly made of amylose in this double mutant. Indeed, the *gbss1*- *ss1*- *ss2*- triple mutant is still under construction and not yet available for this study. Nevertheless, because the  $\lambda_{\max}$  with iodine of the low mass fraction in the *ss1*- *ss2*- double mutant is well above 600 nm (indeed close to 650 nm), it is highly probable that this fraction also defines true amylose.

These data suggest that SS1 and SS2 activity both can influence the activity of GBSS1. The latter enzyme appears to be increased in activity compared to normal when SS2 and SS1 are missing, because the total amount of amylose in the leaves is elevated. The *ss1*- *ss3*- double mutant also had elevated amylose as a percentage of total glucan in the starch granules, however, in this instance, the amount of amylose per mg leaf fresh weight was not changed from normal. Thus, the increased abundance of amylose in granules in *ss1*- *ss3*- plants results from a reduction in amylopectin content as opposed to an elevation of the amylose level. The content of GBSS1 within the starch granule was determined by SDS-PAGE analysis of granule bound proteins (see Supplementary Fig. S5 at JXB online). GBSS1 content was equivalent in WT and SSs mutant lines.

The wavelength of maximum absorbance ( $\lambda_{\max}$ ) of the iodine–amylopectin complex was altered in all mutant lines compared with the wild type, and this effect was enhanced in both the *ss1*- *ss2*- and *ss1*- *ss3*- double mutants (Fig. 3). This result indicates a change in amylopectin structure, with the higher  $\lambda_{\max}$  value indicative of longer chains on average than are present in the wild type.

The linear chain length distribution profile of amylopectin was established for each line. Amylopectin was purified by size exclusion chromatography, then all  $\alpha(1\rightarrow6)$  branch linkages were hydrolysed by *Pseudomonas* isoamylase and the linear glucans released were separated and quantified by high performance anion exchange chromatography with pulsed amperometric detection (HPAEC-PAD). The molar ratio of chains with a particular number of glucose units was then determined as a function of the total number of chains in the population (Fig. 4). The results for *ss1*-, *ss2*- or *ss3*- single mutant lines agreed with previously published results (Delvallé et al., 2005; Zhang et al., 2005, 2008). Such analysis of *ss1*- *ss2*- and *ss1*- *ss3*- lines allows estimation of the function of SS3 or SS2 alone as the primary determinant of amylopectin chain length distribution, considering that *ss4*- mutations have little effect on amylopectin structure in *Arabidopsis* leaves (Roldán et al., 2007; Szydlowski et al., 2009). Both double mutant starches have lost the peak modality that is centred at DP 21, which is a characteristic of *ss1*- mutants and specific to lines bearing that deficiency (Fig. 4). This fact is indicated by the peak observed at DP 15–22 in difference plots in which the wild-type values

for each DP are subtracted from those of ss1-, ss1- ss3-, or ss1- ss2- starches. SS1, therefore, is necessary to restrict the abundance of chains in the range of approximately DP 15-22. For chains in the range of DP 6-10, which are decreased in abundance in ss1- single mutants, the defect is strongly exacerbated by the additional loss of SS3. The latter enzyme, therefore, appears to partially overlap in function with SS1 in the construction of short linear chains of amylopectin. SS3 acting alone in the ss1- ss2- double mutant has a near normal frequency of chains in the range of DP 5-16.

### **Branch linkage placement**

The effects of altered SS composition on the branching structure of amylopectin were investigated by pretreating with  $\beta$ -amylase prior to standard chain length distribution analysis.  $\beta$ -amylase is an exoamylase that specifically cleaves  $\alpha(1\rightarrow4)$  linkages of  $\alpha$ -glucans starting from their non-reducing ends, progressing towards the internal parts of the glucan and stopping a few residues upstream of an  $\alpha(1\rightarrow6)$  branch. This treatment eliminates outer chains lacking branch linkages (A chains) and, because  $\beta$ -amylase cannot proceed across a branch, reveals the placement of  $\alpha(1\rightarrow6)$  linkages relative to each reducing end as the distribution of residual chain lengths (see Supplementary Fig. S1 at JXB online).

Subtracting the chain length frequencies in untreated amylopectin from those observed after  $\beta$ -amylase digestion reveals whether particular glucans are unbranched and thus external or, alternatively, are branched and thus contribute to the root of one or more clusters. In wild-type amylopectin, the frequencies of short chains of DP 5-9 increase significantly after exoamylase treatment (Fig. 5; CLD of  $\beta$ -limit dextrins are presented in Supplementary Fig. S4 at JXB online). These chains are presumed to derive from the roots of the clusters and indicate a range of 3-7 glucose units for the distance from the reducing end to the distal branch point in such clusters (green and yellow chains in Supplementary Fig. S1 at JXB online). The chains of DP 16-20 accumulating after  $\beta$ -amylase pretreatment are expected to have been produced from longer glucans that span two different clusters (white and red chains in Supplementary Fig. S1 at JXB online). The method was then used to test whether the large excess of chains of DP 15-22 in the ss1-, ss1- ss2-, and ss1- ss3- mutants compared with the wild type (Fig. 4) derive from altered architecture so that there are more inter-cluster chains or, alternatively, are abnormally long outer chains. The  $\beta$ -amylase treatment effectively removed all of the excess DP 15-22 chains from these mutant amylopectins (Fig. 5), indicating that they are external A chains as had been previously demonstrated for the ss1- single mutant (Delvallé et al., 2005). This analysis applied to the ss2- and ss3- lines revealed that the frequency of internal chains spanning two clusters was not changed by either mutation (Fig. 5).

The same approach was used to test whether the DP 7-9 chains, that are much more abundant in ss2- mutant starch than in wild-type starch (Fig. 4), are external or branched and thus internal. Such chains were decreased in abundance after  $\beta$ -amylase treatment. This is particularly evident for DP 8 glucans (Fig. 5) that are increased to the greatest extent in ss2- mutants. These results demonstrate that abnormally short outer chains accumulate in the absence of SS2.



Analysing the  $\beta$ -amylolysis data as a difference plot in which the frequency for each DP from wild-type starch was subtracted from that of the mutant revealed a connection between SS function and branch linkage placement. In this analysis, if only chain length distribution is modified, and not branch placement, then no change is expected between the profiles of the wild type and the mutant after  $\beta$ -amylolysis. Conversely, if branch linkages placement is altered, then the chain length profile after  $\beta$ -amylolysis should be different between the wild type and the mutants. Such analyses revealed only slight differences between the wild type and any single mutant (Fig. 6). Thus, the placement of branches relative to the reducing end is normal in each single mutant and no individual SS function is necessary for normal structure in this aspect of starch architecture. In the ss1- ss2- and ss1- ss3- double mutants, however, major alterations of the difference plots were observed that were not anticipated from the profiles of the corresponding single mutants. In starch from both double mutant lines the frequency of linear glucans of DP =10 was increased and the frequency of chains in the range of DP 13–29 was reduced, both to a large extent (Fig. 6). This indicates that the internal structure of amylopectin was strongly affected by the simultaneous elimination of the two SS classes. Specifically, the increase in residual chains of DP 10 or less after  $\beta$ -amylolysis indicates that, in the double mutants, the distribution of placements between the reducing end and the first branch was reduced within the cluster roots. Furthermore, the decrease in residual chains in the range of DP 13–29 reveals that the number of glucans that span multiple clusters is reduced, and/or that the length of spans between clusters is shortened. The same behaviour was observed for the amylopectin of the ss1- ss2- ss3- triple mutant (Szydowski et al., 2009) treated in the same way (Fig. 6).

The number of branches in amylopectin (Table 2) was deduced from CLD analysis for each sample (Fig. 4; Szydowski et al., 2009) as described in equation 1. Since the number of DP <5 and DP >40 glucans was very low in all samples analysed in this report, the number of branches was estimated as follow:

$$\frac{100}{100 + \sum_{i=5}^{40} DP_i\% \times (DP_i - 1)}$$

where DP<sub>i</sub>% is the percentage of the glucan within the population analysed and DP<sub>i</sub> is the length of the glucan. The ratio of branches was not significantly modified in the different mutants analysed in this study and was in the range of branching level commonly described for amylopectin. In comparison, the same method applied to glycogen and isa1- isa3- pu1- residual amylopectin gave a ratio of branches above 8.2% in both instances, which was expected for these polymers.

Note that in this study, the number of A and B1 chains was not considered because maltose produced by  $\beta$ -amylase was not removed before debranching and subsequent analysis by HPAEC-PAD. It was thus impossible to determine the frequency of these short chains of amylopectin as already described (Bertoft et al., 2008; Pérez and Bertoft, 2010).

Taken together these data indicate that the mechanism for determination of branch placement, presumably executed by BE and/or SBE, is influenced by SSSs.

### Starch granule morphology

The impact of the mutations on the morphology of the starch granules was assessed by both scanning (SEM) and transmission (TEM) electron microscopy (Fig. 7). The double mutants were compared to the wild type and each single mutant all in the same genetic background and growth conditions, so as to minimize potential environmental effects. Granules were purified from plants harvested 3 h prior to onset of the dark phase in the LD growth regime. Wild-type granules were flattened discs with smooth surfaces and diameters of 2-4  $\mu\text{m}$ , and this morphology was not altered noticeably in the *ss1*- mutant. Granules from the *ss2*- mutant, by comparison, typically had curved shapes and appear to be larger than the wild type on average. Leaves from the *ss3*- mutant contained many very small granules less than 1  $\mu\text{m}$  in diameter, which were seen only rarely in the wild type. The *ss3*- mutant granules occasionally were curved, as observed for the *ss2*- line.

Both double mutant lines produced starch granules that were less severely abnormal than those of the *ss2*- or *ss3*- single mutants (Fig. 7). Granules from the *ss1*- *ss2*- double mutant were regular in shape compared with the highly variable *ss2*- granules. The *ss1*- *ss2*- double mutant granules were still abnormal however, because curved shapes were frequent and they were noticeably larger, on average, than the wild type. In the *ss1*- *ss3*- mutant the granule size was, on average, smaller than that of the wild type but larger than that of the *ss3*- single mutant. The very small granules found in the *ss3*- line were much less frequent in the *ss1*- *ss3*- mutant.

## **Discussion**

This study was undertaken to define further the functional redundancies between three of the four soluble starch synthases of chloroplast-containing organisms, specifically SS1, SS2, and SS3. Strict conservation of all three enzyme classes implies a selectable function in these organisms, and indeed specific deficiencies in starch structure were observed when any one enzyme was absent (Delvallé et al., 2005; Zhang et al., 2005, 2008). Crystalline starch still accumulates, however, in normal or near-normal quantity in any single SS1, SS2, or SS3 mutant tissue that has been studied. Some extent of functional redundancy is thus obvious, as demonstrated directly by previous work in potato and *Arabidopsis* (Edwards et al., 1999; Lloyd et al., 1999a; Jobling et al., 2002; Zhang et al., 2008). In those instances starch accumulation and structure in lines with simultaneously reduced SS2 and SS3 did not result from the simple addition of the phenotypes observed in single mutant lines. The apparent discrepancy between selection and redundancy must be explained by, as yet not understood, interconnections between the various activities that build amylopectin and determine its molecular architecture, thus generating crystalline starch. Functional interdependence is likely to exist not only among the SSs, but also between SS and BE and DBE. The double mutant combinations studied here provide further insight into the roles of functional redundancy among SSs and, in addition, reveal that the placement of branch linkages is influenced by SS activity.

## **Compensatory mechanisms for the determination of starch levels**

A possible contributing factor for the selection of multiple SSs is plasticity in the pathway in order to accommodate fluctuation in ADP-glucose levels through substrate affinity for this precursor molecule. Compensation for starch content is obvious from the finding that, in SD growth conditions, the *ss1- ss2-* double mutant, rather than being severely deficient in starch content, actually accumulates significantly more starch than does the *ss2-* single mutant (Fig. 2). Discounting the unlikely possibility that glucan degradation is deficient in the double mutant, it appears that a remaining SS is more active when SS1 is absent. GBSS1 is probably the enzyme activity affected, because of the strong increase in the net low mass fraction (the fraction that behaves like amylose when subjected to size exclusion chromatography on Sepharose® CL-2B matrix) content in the double mutant (Table 2). Total low mass fraction content normalized to leaf fresh weight, is elevated by 66% in the *ss1- ss2-* line compared with the wild type, and by 43% in the *ss2-* single mutant. This low mass fraction is lacking in a *gbss1- ss2-* double mutant (see Supplementary Fig. S3 at JXB online), confirming that GBSS1 is necessary to produce such high levels of this fraction in this mutant that thus could be considered as true amylose (i.e. under the control of GBSS1 activity). Although it is not yet possible to conclude that the low mass fraction in the *ss1- ss2-* double mutant defines true amylose (the *gbss1- ss1- ss2-* triple mutant is under selection in our laboratory) we have several lines of evidence that suggest that this fraction also defines amylose (very high  $\lambda_{max}$  with iodine for instance).

Compensation in starch level mediated by GBSS1 could be explained by altered ADP-glucose availability. GBSS1 protein abundance can be ruled out as an explanation because this parameter is unchanged in *ss2-* single and *ss1- ss2-* double mutants compared with the wild type (see Supplementary Fig. S5 at JXB online). Another possibility is that modified amylopectin structure alters GBSS1 activity by offering a different glucan substrate for elongation. However, total amylose content is significantly elevated in both the *ss2-* and *ss1- ss2-* mutants, even though amylopectin structure is distinct in these two lines with regard to chain length distribution and branch linkage placement (Figs. 4, 6). It is unlikely that two such different amylopectin structures could elevate GBSS activity in the same way. Availability of ADP-glucose is a potential explanation because of differences in apparent affinity for this substrate between GBSS and other SSs. Most soluble SSs that have been studied display a  $K_m$  for ADP-glucose below 1 mM (Fontaine et al., 1993; Imparl-Radosevich et al., 1999; Delvallé et al., 2005), whereas the  $K_m$  of GBSS1 is 5 mM or more (Delrue et al., 1992; Lloyd et al., 1999b). The lack of both SS1 and SS2 could reduce the use of ADP-glucose, thus increasing substrate available to GBSS1 and allowing it to synthesize amylose to an extent that compensates for the reduction in amylopectin.

Elevated total amylose content occurs only in the absence of SS2 and the presence of SS3. The compensation mechanism evidently is not possible in *ss2- ss3-* double mutants or the triple mutant *ss1- ss2- ss3-* line, because, in those instances, the total starch level is drastically reduced including a large decrease in the total amylose content in leaves (Zhang et al., 2008; Szydlowski et al., 2009). Amylopectin alterations are extreme in the multiple mutant combinations in which SS3 is absent (Szydlowski et al., 2009; Zhang et al., 2008), so it is unlikely that the crystalline matrix necessary to support GBSS1 activity can form and thus amylose levels cannot be elevated. Why total amylose levels cannot increase in *ss1-* mutants

to compensate for a loss of SS1 activity is not clear, but could be related again to the availability of ADP-glucose.

Compensation for loss of a particular SS activity is also indicated by enzymatic assay of total soluble extracts. In *ss3*- single mutant lines, complete loss of SS3 protein has no effect on the total SS activity in soluble extracts. However, when coupled with the *ss1*- mutation, loss of SS3 has a major effect (Table 1). A possible explanation is that SS1 activity is elevated in the absence of SS3. This is consistent with the analysis of SS activity in maize endosperm extracts, in which loss of SS3 resulted in elevated total activity rather than the expected decrease (Singletary et al., 1997). In *Arabidopsis*, increased SS1 activity is probably not due to increased expression of the structural gene of SS1 since transcriptomic analysis of the *ss3*- mutant failed to show any changes in starch synthase genes expression level (SS1, SS2, SS4, and GBSS1 genes; see Supplementary Fig. S6 at JXB online). Similar results were observed for the *ss2*- mutations, which by itself had no effect on total SS activity, but when coupled with *ss1*- in the double mutant line caused a large decrease. Thus, SS1 appears to provide more activity than normal in extracts lacking either SS2 or SS3. A possible explanation for this phenomenon is that SS2 and SS3 both function as negative regulators of SS1 activity. The fact that total SS activity is unaltered from the wild-type level in *ss2*- *ss3*- mutant lines (Zhang et al., 2008) is consistent with this hypothesis. Elevation of SS1 activity in extracts does not translate into fully redundant *in vivo* function, because starch structure is altered in any single or double mutant line. Compensatory activities, however, could contribute to selection of multiple SS classes during plant evolution. It must be stressed that SS2 elongation activity was never detected in *Arabidopsis* leaves in this study but also in previous studies (Delvallé et al., 2005; Zhang et al., 2008). It is still unclear why SS2 activity remains undetectable in *Arabidopsis* leaves. Thus compensation of SS activity in the different mutants should be considered here as compensating mechanism between SS1 and SS3 only.

### **SS redundancy and specificity in construction of amylopectin**

Chain length distribution analyses show that SS3 is partially redundant with SS1 for construction of the shortest chains in amylopectin, of DP 8-11. The deficiency in frequency of such chains that is observed in the *ss1*- single mutant is exacerbated in the *ss1*- *ss3*- double mutant and is far more than the sum of the individual phenotypes (Fig. 4). Thus, SS3 function either directly or indirectly leads to formation of short chains, although this activity cannot completely replace the need for SS1 to produce normal amylopectin structure. SS3 is also known to be partially redundant in function with SS2 for the generation of chains of DP 15-22 (Zhang et al., 2008), indicating that the SS3 has a broad specificity that is able to perform at least some of the functions of SS1 and SS2. Consistent with this conclusion is the observation that the frequency of chains up to DP 15 is near normal in the *ss1*- *ss2*- mutant, relative to the extreme changes seen in other double mutant combinations (Fig. 4).

SS1 appears to be unique in some function that is necessary to produce the normal distribution of chain lengths in the region of DP 15-21. Wild-type *Arabidopsis* leaf starch clearly exhibits a bimodal distribution of chain lengths with one optimum at DP 12 and another at DP 21. The second mode in the distribution is lost if SS1 is absent and the double mutant results reveal that this function absolutely cannot be replaced by SS2 or SS3. The reason that SS1

affects synthesis of DP 14-21 chains is not clear because the activity of this enzyme decreases rapidly with increasing DP of the substrate, to virtually none at DP 12 (Commuri and Keeling, 2001). SS1 thus appears to have a negative affect on the activity of either SS2 or SS3 that prevents elongation of its own glucan product.

### **Branch linkage placement is altered in the SS double mutants**

Treatment of wild-type and mutant amylopectin with  $\beta$ -amylase prior to debranching for chain length distribution analysis revealed that the core structure of this polymer is severely modified when more than one SS class is absent. As described in a previous section, the chain length distribution after  $\beta$ -amylolysis reveals the distribution of the number of glucose units from the reducing end of each chain to the outermost  $\alpha(1\rightarrow6)$ -branched residue. This parameter is essentially unaffected in any of the single mutant starches (Fig. 6), however, all the double mutants as well as the ss-1 ss2- ss3- triple mutant have substantially shifted that distribution to a smaller length range compared to the wild type (Fig. 6). This result demonstrates that the placement of branch linkages is changed as the result of SS reduction, such that at least two SSs are required for normal architecture.

Activities of either BEs or DBEs, or a combination thereof, could be influenced by the presence of SS proteins. BEs require glucans of sufficient length in order to create branches through intra- or intermolecular rearrangement (Guan and Preiss, 1993; Guan et al., 1994). One possibility is that potential substrates of BE are altered as the result of reduced SS activity. Alternatively, the effects of SS deficiency on BE function could be indirect owing to interactions between the proteins. Multiple protein complexes including both BE and SS1, SS2, and SS3 have been demonstrated to occur in maize and wheat (Hennen-Bierwagen et al., 2008, 2009; Tetlow et al., 2008). Presuming such interactions occur in leaf tissue, the SS-BE interactions in one or more physical complexes could affect the outcome of branch placement. At least two SSs must be missing in order to observe this effect, which could indicate that multiple complexes function to co-ordinate branch placement; such behaviour was already described in yeast for the pathway of proteins secretion (Rothblatt et al., 1989). Finally, DBEs must also be considered as a factor that could be influenced by SSs in determining the ultimate distribution of branch linkage placement. In this view, hydrolysis of some branch linkages after they have been placed by a BE is necessary to achieve normal amylopectin structure, so that reduced DBE activity could be responsible for the shorter distribution of the number of glucose units from the reducing end to the outer branch point in the double mutants lacking multiple SS.

### **Abnormal amylopectin structure can cause altered granule morphology**

The determinants of starch granule morphology are not well understood, although high amylose content has been proposed to cause abnormal granule shapes. However, data from this study suggest that the distorted morphology of ss2- mutant starch granules results from abnormal amylopectin structure rather than high amylose content. The relevant observation is that the amylose content of starch granules from the ss1- ss2- double mutant is even higher than that of the ss2- single mutant. The morphological abnormality of the double mutant granules, however, is noticeably less severe than that of the ss2- single mutant (Fig. 7). The CLD profiles of both ss2- and ss1- ss2- mutants are distinctly different for glucan chains of DP <15, such that the frequency of short chains in the range DP 7-9 is strongly increased in the

single mutant (Fig. 4). These very short glucans, whose synthesis is under the control of SS1 in the absence of SS2, are mostly external A and B1 chains (see Supplementary Fig. S1 at JXB online) because they are susceptible to degradation by  $\beta$ -amylase (Fig. 5). Their presence could disturb the build up of the starch granule structures because these glucans are too short to serve as substrates for BEs (Guan and Preiss, 1993; Guan et al., 1994, 1997). The lamellar organization of amylopectin would then be disrupted in a manner unique to the *ss2*- mutant, leading to structural flaws that amplify during granule expansion and result in grossly misshapen starch. These observations support the explicit assumption that the fine structure of amylopectin determines granule morphology through higher order structural assembly.

### **Acknowledgments**

We express our gratitude to Emilie Perrin for her excellent technical assistance in microscopy analysis. We acknowledge Adeline Courseaux for her technical assistance. Many thanks to Maria Cecilia Arias who provides transcriptomics data. This work was partly supported by ANR Génoplande (GPLA0611G to CDH, NS, and VP), the European Union-FEDER and the Région Nord Pas de Calais (ARCir PlantTEQ5 to CDH, NS, and FW), and by award no. DBI-0209789 from the National Science Foundation to AMM and by grants BIO2009-07040 from the Comisión Interministerial de Ciencia y Tecnología and the European Union-FEDER, and by grant P09-CVI-4704 from Junta de Andalucía to AM. PR was supported by an FPU grant from the Spanish Ministry of Education.

## References

↵ Ball SG, van de Wal MHB, Visser RGF

Progress in understanding the biosynthesis of amylose. *Trends in Plant Science* 1998;3:462-467.

↵ Bertoft E, Piyachomkwan K, Chatakanonda P, Sriroth K

Internal unit chain composition in amylopectins. *Carbohydrate Polymers* 2008;74:527-543.

↵ Buleon A, Colonna P, Planchot V, Ball S

Starch granules: structure and biosynthesis. *International Journal of Biological Macromolecules* 1998;23:85-112.

↵ Commuri PD, Keeling PL

Chain-length specificities of maize starch synthase I enzyme: studies of glucan affinity and catalytic properties. *The Plant Journal* 2001;25:475-486.

↵ Dauvillee D, Kinderf IS, Li Z, Kosar-Hashemi B, Samuel MS, Rampling L, Ball S, Morell MK

Role of the *Escherichia coli* glgX gene in glycogen metabolism. *Journal of Bacteriology* 2005;187:1465-1473.

↵ Delrue B, Fontaine T, Routier F, Decq A, Wieruszeski JM, Van Den Koornhuysen N, Maddelein ML, Fournet B, Ball S

Waxy *Chlamydomonas reinhardtii*: monocellular algal mutants defective in amylose biosynthesis and granule-bound starch synthase activity accumulate a structurally modified amylopectin. *Journal of Bacteriology* 1992;174:3612-3620.

↵ Delvallé D, Dumez S, Wattebled F, et al

Soluble starch synthase I: a major determinant for the synthesis of amylopectin in *Arabidopsis thaliana* leaves. *The Plant Journal* 2005;43:398-412.

↵ Deschamps P, Moreau H, Worden AZ, Dauvillee D, Ball SG

Early gene duplication within chloroplasts and its correspondence with relocation of starch metabolism to chloroplasts. *Genetics* 2008;178:2373-2387.

↵ Dumez S, Wattebled F, Dauvillee D, Delvalle D, Planchot V, Ball SG, D'Hulst C

Mutants of *Arabidopsis* lacking Starch Branching Enzyme II substitute plastidial starch synthesis by cytoplasmic maltose accumulation. *The Plant Cell* 2006;18:2694-2709.

↵ Edwards A, Fulton DC, Hylton CM, Jobling SA, Gidley M, Rössner U, Martin C, Smith AM

A combined reduction in activity of starch synthases II and III of potato has novel effects on the starch of tubers. *The Plant Journal* 1999;17:251-261.

↵ Fontaine T, D'Hulst C, Maddelein M, Routier F, Pepin T, Decq A, Wieruszkeski J, Delrue B, Van den Koornhuysen N, Bossu J

Toward an understanding of the biogenesis of the starch granule. Evidence that *Chlamydomonas* soluble starch synthase II controls the synthesis of intermediate size glucans of amylopectin. *Journal of Biological Chemistry* 1993;268:16223-16230.

↵ Guan H, Li P, Imparl-Radosevich J, Preiss J, Keeling P

Comparing the properties of *Escherichia coli* branching enzyme and maize branching enzyme. *Archives of Biochemistry and Biophysics* 1997;342:92-98.

↵ Guan HP, Baba T, Preiss J

Expression of branching enzyme I of maize endosperm in *Escherichia coli*. *Plant Physiology* 1994;104:1449-1453.

↵ Guan HP, Preiss J

Differentiation of the properties of the branching isozymes from maize (*Zea mays*). *Plant Physiology* 1993;102:1269-1273.

↵ Hennen-Bierwagen TA, Lin Q, Grimaud F, Planchot V, Keeling PL, James MG, Myers AM

Proteins from multiple metabolic pathways associate with starch biosynthetic enzymes in high molecular weight complexes: a model for regulation of carbon allocation in maize amyloplasts. *Plant Physiology* 2009;149:1541-1559.

↵ Hennen-Bierwagen TA, Liu F, Marsh RS, Kim S, Gan Q, Tetlow IJ, Emes MJ, James MG, Myers AM

Starch biosynthetic enzymes from developing maize endosperm associate in multisubunit complexes. *Plant Physiology* 2008;146:1892-1908.

↵ Hizukuri S

Polymodal distribution of the chain lengths of amylopectin, and its significance. *Carbohydrate Research* 1986;147:342-347.

↵ Imparl-Radosevich JM, Nichols DJ, Li P, McKean AL, Keeling PL, Guan H

Analysis of purified maize starch synthases IIa and IIb: SS isoforms can be distinguished based on their kinetic properties. *Archives of Biochemistry and Biophysics* 1999;362:131-138.

↵ Jobling SA, Westcott RJ, Tayal A, Jeffcoat R, Schwall GP

Production of a freeze-thaw-stable potato starch by antisense inhibition of three starch synthase genes. *Nature Biotechnology* 2002;20:295-299.

↵ Laby RJ, Kim D, Gibson SI



The ram1 mutant of Arabidopsis exhibits severely decreased  $\beta$ -amylase activity. Plant Physiology 2001;127:1798-1807.

↵ Liu F, Makhmoudova A, Lee EA, Wait R, Emes MJ, Tetlow IJ

The amylose extender mutant of maize conditions novel protein–protein interactions between starch biosynthetic enzymes in amyloplasts. Journal of Experimental Botany 2009;60:4423-4440.

↵ Lloyd JR, Landschütze V, Kossmann J

Simultaneous antisense inhibition of two starch-synthase isoforms in potato tubers leads to accumulation of grossly modified amylopectin. Biochemical Journal 1999 a;338:515-521.

Lloyd JR, Springer F, Buléon A, Müller-Röber B, Willmitzer L, Kossmann J

The influence of alterations in ADP-glucose pyrophosphorylase activities on starch structure and composition in potato tubers. Planta 1999 b;209:230-238.

↵ Myers AM, Morell MK, James MG, Ball SG

Recent progress toward understanding biosynthesis of the amylopectin crystal. Plant Physiology 2000;122:989-997.

↵ Pérez S, Bertoft E

The molecular structures of starch components and their contribution to the architecture of starch granules: a comprehensive review. Starch–Stärke 2010;62:389-420.

↵ Roldán I, Wattedled F, Lucas MM, Delvallé D, Planchot V, Jiménez S, Pérez R, Ball S, D'Hulst C, Merida Á

The phenotype of soluble starch synthase IV defective mutants of Arabidopsis thaliana suggests a novel function of elongation enzymes in the control of starch granule formation. The Plant Journal 2007;49:492-504.

↵ Rothblatt JA, Deshaies RJ, Sanders SL, Daum G, Schekman R

Multiple genes are required for proper insertion of secretory proteins into the endoplasmic reticulum in yeast. Journal of Cell Biology 1989;109:2641-2652.

↵ Singletary GW, Banisadr R, Keeling PL

Influence of gene dosage on carbohydrate synthesis and enzymatic activities in endosperm of starch-deficient mutants of maize. Plant Physiology 1997;113:293-304.

↵ Szydłowski N, Ragel P, Raynaud S, et al

Starch granule initiation in Arabidopsis requires the presence of either class IV or class III starch synthases. The Plant Cell 2009;21:2443-2457.

↵ Tetlow IJ, Beisel KG, Cameron S, Makhmoudova A, Liu F, Bresolin NS, Wait R, Morell MK, Emes MJ

Analysis of protein complexes in wheat amyloplasts reveals functional interactions among starch biosynthetic enzymes. *Plant Physiology* 2008;146:1878-1891.

↵ Wattedled F, Dong Y, Dumez S, et al

Mutants of *Arabidopsis* lacking a chloroplastic isoamylase accumulate phytyloglycogen and an abnormal form of amylopectin. *Plant Physiology* 2005;138:184-195.

↵ Wattedled F, Planchot V, Dong Y, Szydowski N, Pontoire B, Devin A, Ball S, D'Hulst C

Further evidence for the mandatory nature of polysaccharide debranching for the aggregation of semicrystalline starch and for overlapping functions of debranching enzymes in *Arabidopsis* leaves. *Plant Physiology* 2008;148:1309-1323.

↵ Zeeman SC, Northrop F, Smith AM, ap Rees T

A starch-accumulating mutant of *Arabidopsis thaliana* deficient in a chloroplastic starch-hydrolysing enzyme. *The Plant Journal* 1998;15:357-365.

↵ Zeeman SC, Tiessen A, Pilling E, Kato KL, Donald AM, Smith AM

Starch synthesis in *Arabidopsis*. Granule synthesis, composition, and structure. *Plant Physiology* 2002;129:516-529.

↵ Zeeman SC, Smith SM, Smith AM

The diurnal metabolism of leaf starch. *Biochemical Journal* 2007;401:13-28.

↵ Zhang X, Myers AM, James MG

Mutations affecting starch synthase III in *Arabidopsis* alter leaf starch structure and increase the rate of starch synthesis. *Plant Physiology* 2005;138:663-674.

↵ Zhang X, Szydowski N, Delvallé D, D'Hulst C, James MG, Myers AM

Overlapping functions of the starch synthases SSII and SSIII in amylopectin biosynthesis in *Arabidopsis*. *BMC Plant Biology* 2008;8:96.

## Figure captions

Figure 1. Zymograms of starch-modifying activities. (A) Zymogram of soluble starch synthases activities on polyacrylamide gel containing 0.3% (w/v) of rabbit liver glycogen. After migration, the gel was incubated overnight with 1 mM ADP-glucose. Activities were revealed by iodine staining. (B) Zymogram of starch-modifying activities on a polyacrylamide gel containing 0.3% (w/v) of potato starch. Activities were revealed by iodine staining after overnight incubation, as described in the Materials and methods. Visible activities were previously identified (Delvallé et al., 2005). (C) Zymogram of  $\beta$ -limit dextrin-modifying activities. The gel contains 0.3% (w/v) of maize  $\beta$ -limit dextrin. Visible activities were previously identified (Wattebled et al., 2008). (D) Zymogram of pullulanase activity on a gel containing 0.1% (w/v) of red pullulan. (E) Zymogram of phosphoglucomutase activities. Activities were revealed by specific colorimetric reaction as described in the Materials and methods.

Figure 2. Starch contents in the leaves of double mutants, parental lines, and wild-type plants. Starch content was determined at the end of the day, in plants cultivated under 12/12 h light/dark or 16/8 h light/dark photoperiods. Plant leaves were destained in 80% ethanol (v/v) and ground in 0.2 N KOH. Starch was dissolved by boiling and glucose was quantified by an enzymatic method after the polymer was completely hydrolysed by amyloglucosidase. The starch contents in mutant plants are expressed as a percentage compared with the amount of starch in the wild-type reference. The name of each line is indicated at the inner base of the bars.

Figure 3. Fractionation of starch polysaccharides by size exclusion chromatography. Starch was purified from plant leaves harvested at the end of the light period, and dissolved by boiling in DMSO. Amylose and amylopectin were separated on Sepharose<sup>®</sup> CL-2B matrix equilibrated with 10 mM NaOH and 0.3 ml fractions were collected. Maximum absorption wavelength ( $\lambda_{\max}$ , right y-axis in nm) and maximum OD (OD $_{\max}$  left y-axis) of the iodine–glucan complex were determined in each fraction after the addition of I<sub>2</sub>/KI solution.  $\lambda_{\max}$  (black dots) and OD $_{\max}$  (continuous line) are displayed. The elution volume is indicated on the x-axis.  $\lambda_{\max}$  of amylopectin is indicated at the top of the peak for each type of starch.

Figure 4. Chain length distribution of amylopectin-forming glucans. After purification on a Sepharose CL-2B column, amylopectin was hydrolysed with commercial isoamylase from *Pseudomonas* sp. Digestion products were separated according to their degree of polymerization and quantified by HPAEC-PAD. The relative amount (bars) of each type of glucan (x-axis) is expressed as a percentage of the total number of chains presented in the figure (for instance, glucans of DP12 in the WS profile define 7% of the total number of glucans ranging from DP5 to DP40). A black line, superposed on each mutant profile, displays the difference between the mutant and wild-type profiles.

Figure 5. Resolution of external and internal glucan chains in amylopectin. Purified amylopectin from the indicated genotypes was digested to completion with  $\beta$ -amylase and then completely debranched by treatment with isoamylase. Chain length distributions of the resulting glucans were then determined. Difference plots were calculated by subtracting the mole% of each chain length in intact amylopectin (Fig. 4) from the value obtained after  $\beta$ -amylase treatment (CLD profiles of  $\beta$ -limit dextrans are shown in Supplementary Fig S4 at JXB

online). Values greater than 0 indicate internal chains protected by branches, and values less than 0 indicate unbranched, external chains.

Figure 6. Comparison of outermost branch placement in glucan chains between mutant and wild-type amylopectin. Difference plots were obtained by subtracting the chain length distribution of wild-type amylopectin following  $\beta$ -amylase treatment from the corresponding value obtained from the indicated mutant amylopectin.

Figure 7. Transmission electron microscopy and scanning electron microscopy analysis of starch granules extracted 3 h before dark. The granules were purified by isopicnic centrifugation on a density gradient of Percoll<sup>®</sup>. (A) Scanning electron microscopy pictures of purified starch granules. (B) Transmission electron microscopy pictures of starch granules ultrathin sections.

Table 1

Table 1.

## Enzyme activities in total soluble leaf extracts

Activity	Genotype					
	WS	<i>ss1-</i>	<i>ss2-</i>	<i>ss3-</i>	<i>ss1- ss2-</i>	<i>ss1- ss3-</i>
SS	100	50±8.8	100.3±5.1	92.7	25.4	9.8±4.5
SBE	136.2±10.6	144.5±14.8	118.6±17.4	161.3±3.4	171.3±23.4	191.1±12.9
AGPase-3PGA	3.5±0.8	3.1±1.6	3.7±1.4	3.4±1.6	4.2±0.9	5±1
AGPase+3PGA	12.4±2.1	11.1±1.7	13.8±3.5	12.2±2.6	15.2±1.8	15.2±5
PUL	7.6±1.6	8.1±0.7	7.6±1.5	7.3±0.9	8.7±1.3	8.1±1.6
DE	29.7±0.6	28.2±2.2	27.1±1.1	n.d.	25.6±2.1	n.d.
Maltase	27±1.2	33.5±6.5	27.7±4.2	n.d.	32±5.4	n.d.
AAM	75.8±4.5	77.4±16.2	77±4.6	70.6±13.2	80.7±3	83.1±9.8

Plants were cultivated in a greenhouse under a 16/8 h light/dark photoperiod and leaves were harvested for analysis at the middle of the light phase. SS, soluble starch synthase; SBE, starch branching enzyme; AGPase, ADP-glucose pyrophosphorylase (assayed in the presence or absence of the allosteric activator 3-PGA); PUL, pullulanase; DE, disproportionating enzyme; AAM,  $\alpha$ -amylase. Units are mean nmol product min<sup>-1</sup> mg<sup>-1</sup> protein  $\pm$ SD, except for SS, which is presented as the mean percentage of the wild type value  $\pm$ SD. Three independent biological replicates were assayed for AGPase, PUL, AAM, DE, and maltase. Two such replicates were assayed for SS, except for the *ss3-* genotype that was assayed only once.

Table 2

Table 2.

## Amylose content and amylopectin branching level

Genotype	Replicates	Amylose content		
		Normalized to total starch (wt% $\pm$ SD)	Normalized to leaf mass (mg g <sup>-1</sup> FW)	Branching level <sup>a</sup> (%)
WS (wt)	6	26.7 $\pm$ 2.4	0.62	5.83
<i>ss1</i> -	1	28.0	0.66	6.20
<i>ss2</i> -	6	39.2 $\pm$ 4.5	0.89	6.51
<i>ss3</i> -	2	32.5 $\pm$ 4.5	0.58	6.17
<i>ss1</i> - <i>ss2</i> -	1	48.0	1.03	6.05
<i>ss1</i> - <i>ss3</i> -	3	47.3 $\pm$ 4.2	0.62	5.73
<i>ss1</i> - <i>ss2</i> - <i>ss3</i> -	2	41	0.29	6.88

Plants were cultivated in a greenhouse under a 16/8 h light/dark photoperiod and starch was analysed from leaves harvested at the end of the light phase. Amylose content was determined by quantifying the glucose content in the high molecular weight and low molecular weight fractions separated by gel filtration (see Fig. 3). Replicate numbers refer to independent assays performed with separate groups of plants.

<sup>a</sup> Branching levels were deduced from the CLD profiles established for each genotype presented in Fig. 4. Only glucans of DP between 5 and 40 were used. The number of DP <4 and DP >40 glucans is negligible in the WT and mutant amylopectins analysed here. By comparison, the branching level deduced by the same approach was of 8.28% and 8.25% for *isa1*-*isa3*-*pu1*-amylopectin and glycogen, respectively.

Figure 1

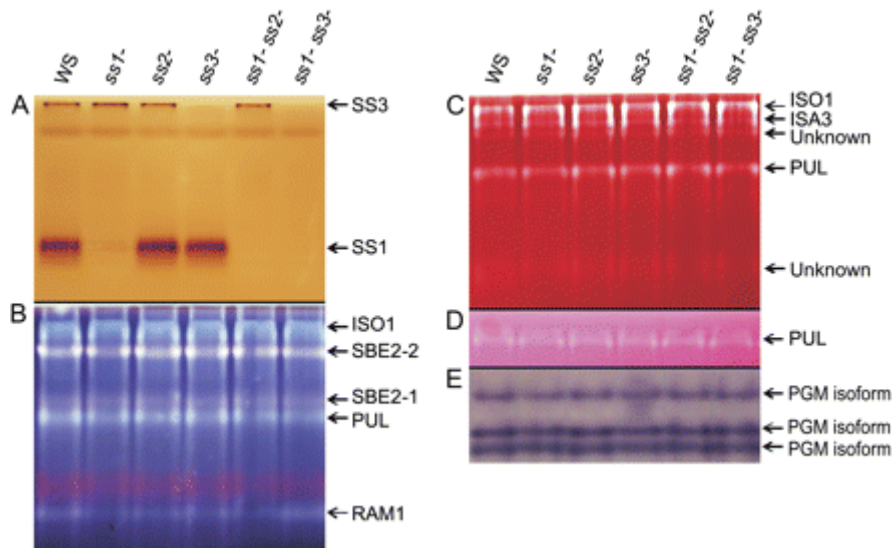


Figure 2

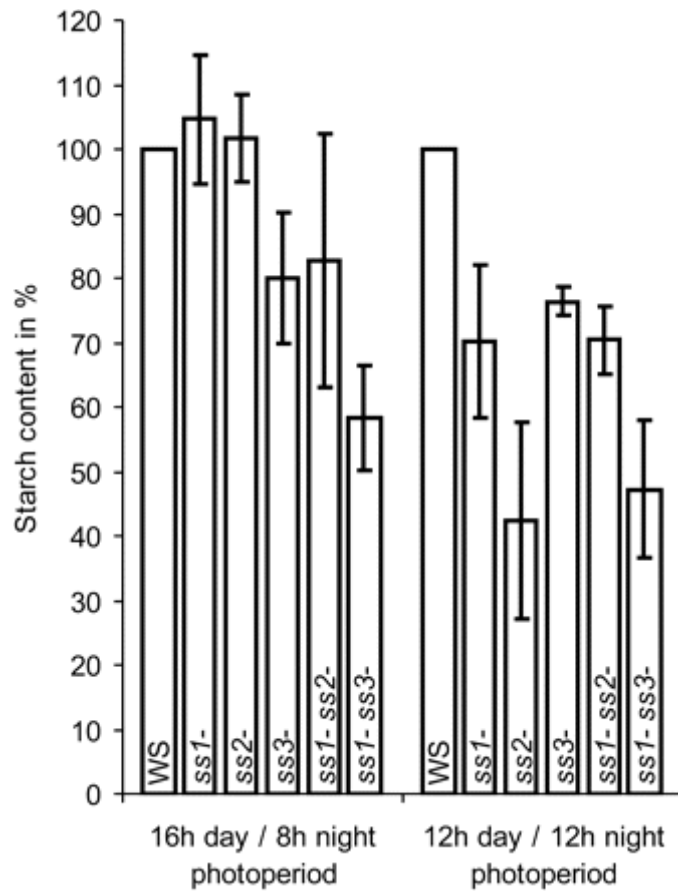




Figure 3

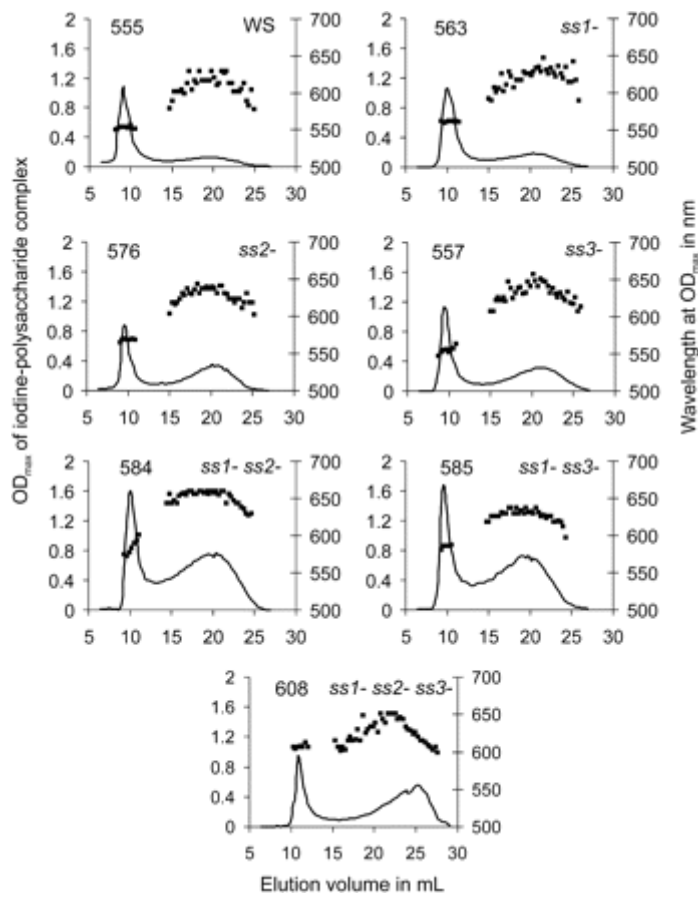


Figure 4

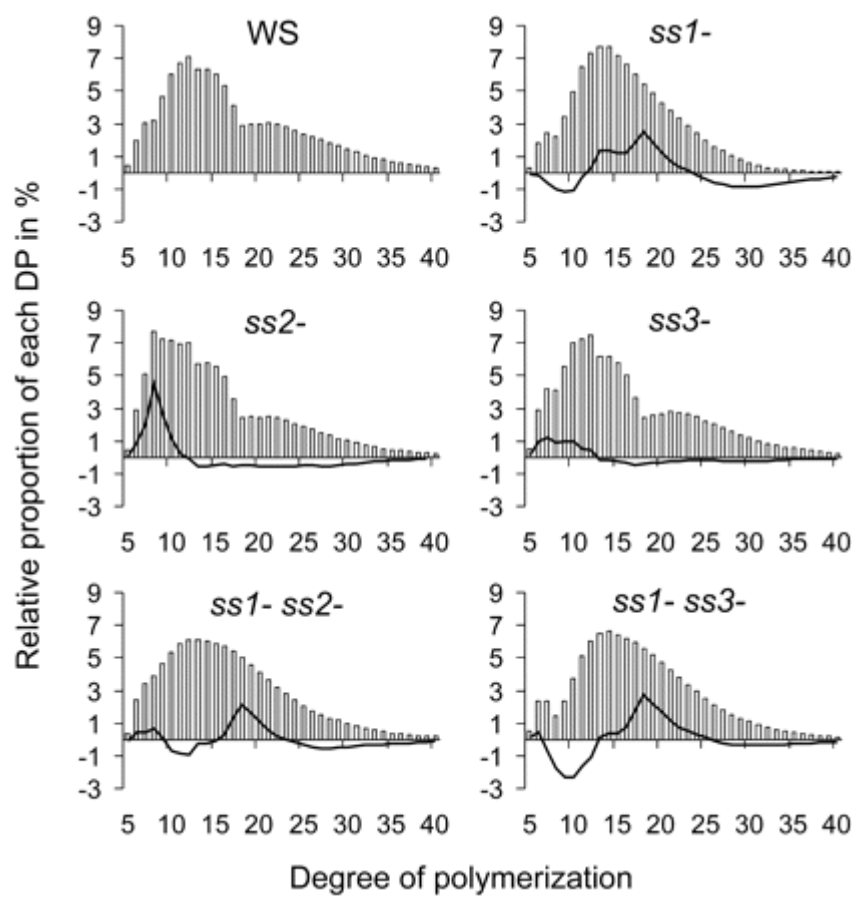


Figure 5

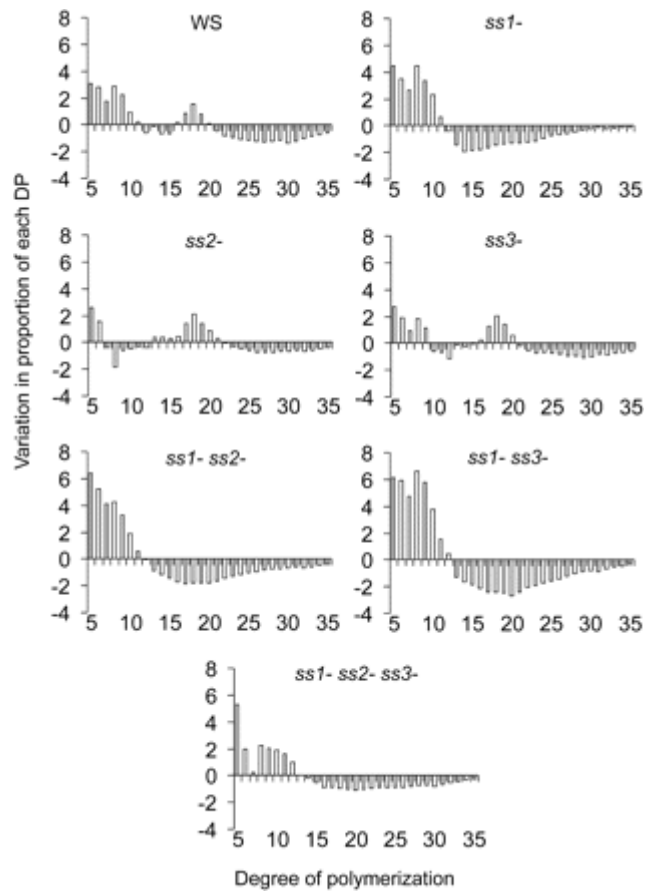


Figure 6

